

## A photocatalytic Activity of a Novel Nanocrystalline SrCO<sub>3</sub> for the Degradation of Erioglucine dye

Ashok V. Borhade\* and Jyoti A. Agashe

Post Graduate Department of Chemistry, H.P.T. Arts and R.Y.K. Science College,

Nashik -05, India.

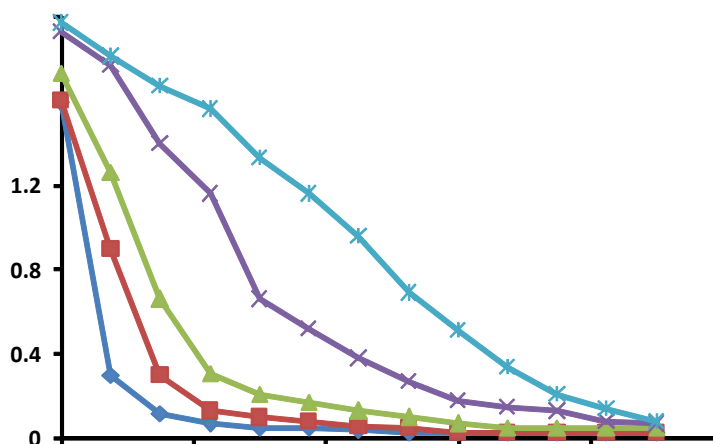
\*E-mail: [ashokborhade2007@yahoo.co.in](mailto:ashokborhade2007@yahoo.co.in).

**Received 5<sup>th</sup> September 2016, Accepted 3<sup>rd</sup> January 2017**

• **Novelty and Highlights:**

- 1- Nanocrystalline SrCO<sub>3</sub> was successfully synthesised hydrothermally.
- 2- SrCO<sub>3</sub> acts as an efficient catalyst for mineralisation of Erioglucine dye.
- 3- Degradation mechanism for Erioglucine dye was established by LCMS analysis.

• **Graphical Abstract:**



## A photocatalytic Activity of a Novel Nanocrystalline SrCO<sub>3</sub> for the Degradation of Erioglaurine dye

Ashok V. Borhade\* and Jyoti A. Agashe

Post Graduate Department of Chemistry, H.P.T. Arts and R.Y.K. Science College,

Nashik -05, India. \*E-mail: [ashokborhade2007@yahoo.co.in](mailto:ashokborhade2007@yahoo.co.in)

Novel recyclable nanocrystalline SrCO<sub>3</sub> photocatalyst has been synthesised by a simple synthetic strategy using hydrothermal precipitation calcination method using Sr(NO<sub>3</sub>)<sub>2</sub> precursor and Ethylene glycol as a surfactant. The synthesized product was characterized by various techniques including Fourier Transform Infra- red (FT-IR) spectroscopy, X-ray powder diffraction (XRD), Ultra-violet Diffused Reflectance (UV-DRS) spectroscopy, Scanning Electron Microscopy (SEM), Transmission Electron Microscopy (TEM) and Bruner –Emmet- Teller (BET) surface area. The photocatalytic efficiency of nanocrystalline SrCO<sub>3</sub> was investigated for the degradation of Erioglaurine dye using visible light irradiation. The recyclability of catalyst was also studied for the degradation and the results obtained have been discussed. The degradation mechanism for Erioglaurine dye has been confirmed by using LC-MS analysis.

*Keywords: Photocatalyst, Nanoparticles, Erioglaurine dye, Recyclability, LC-MS.*

### Introduction

From last many years, photocatalytic degradation has become a challenging technology for the mineralisation of various organic pollutants. This technology has great importance because it's environmentally friendly features, cost effective and low energy utilisation. Photocatalysis technique for wastewater treatment has attracted attention due to the generation of highly potent species such as  $\cdot\text{OH}$  and  $\cdot\text{O}_2$ .

A variety of hazardous pollutants are discharged into the aquatic bodies from several industries [1-3]. Dyes from textile and other commercial dyestuffs have been a focus of environmental remediation in the last few years. Artificial dyes are highly toxic in nature, they develop intense colour and are harmful to the environment. Dyes are organic in nature and it possesses high stability. The newly developed textile dyes alter aquatic life as these dyes are not completely removed during washing process [4,5].

Reports available in literature reveals that most of the work available on photocatalytic degradation is using metal oxides [6-14]. However, there are no reports found in the literature [15-16] on mineralisation of dyes using metal carbonates. Further, it is also observed that most of these investigation deals with the synthesis and characterization using urea as a complexing agent [17-21].

It is important to choose suitable surfactant molecule that acts as templates or shape controlling, directing the formation of a structure toward the desired target arrangement. In the present study SrCO<sub>3</sub> complex structure can be easily generated by using Ethylene glycol as structure directing agent in ambient and low-temperature precipitation experiment. Strontium carbonate is used for devices for various applications [22]. It is also used for manufacturing CTV to absorb electrons resulting from the cathode. Strontium carbonate is also used for making some semiconductors such as BSCCO and also for electroluminescent materials. Hence controlled synthesis of SrCO<sub>3</sub> has attracted much interest [23-25]. During the synthesis of metal carbonates numerous methods have been used by different workers, including monolayer



formation [26-28], ion entrapment [24], and hydrothermal route with various morphologies [29-30].

In connection with our previous reports [11-14] on the catalytic activity of metal oxides, herein we report new  $\text{SrCO}_3$  photocatalyst for the degradation of Erioglaucine dye. Pure phase  $\text{SrCO}_3$  was obtained by heating the precursor at the appropriate temperature. The product obtained was analysed by means of FT-IR, UV-DRS, XRD, SEM, TEM and BET surface area. In the present work, the photocatalytic activity of the as-synthesized  $\text{SrCO}_3$  was performed for the mineralisation of Erioglaucine dye with visible light irradiation. LC-MS technique was used to establish the degradation path for Erioglaucine dye.

## Experimental

**Chemicals** used in the present study were of high quality (AR Grade) and further used without any purification. Strontium nitrate  $\text{Sr}(\text{NO}_3)_2$  (Sigma-Aldrich 99.99%), Sodium hydroxide (NaOH) and Ethylene glycol (Sigma-Aldrich 99.5% pure).

**Synthesis of  $\text{SrCO}_3$**  During the synthesis of  $\text{SrCO}_3$  by hydrothermal route, 1 mmol of strontium nitrate, 2 mmol of NaOH and 0.98 mmol of ethylene glycol were mixed in 100 ml distilled water in a Teflon autoclave and strongly shaken for about 15 min for homogeneous mixing. The obtained reaction mixture was taken in a Teflon-lined stainless steel autoclave (capacity 200 ml) and kept in the oven at  $100^\circ\text{C}$  for one day. After completion of the reaction, a white polycrystalline product of  $\text{SrCO}_3$  was washed and dried in the oven overnight at  $100^\circ\text{C}$ .

**Characterization** The as-prepared sample was characterised by FT-IR using a 8400S (Shimadzu) with wavelength  $4000\text{-}400\text{ cm}^{-1}$ . X-ray diffractometer was used to study phase transfer if any, using DMAX-2500 Rikagu, with  $\text{CuK}\alpha$  radiation ( $\lambda$ )  $1.5406\text{ \AA}$ . The SEM image was taken on a microscope (JSM-6300- JEOL) attached with EDAX spectrophotometer (JED-2300-LA-JEOL). The band gap energy of  $\text{SrCO}_3$  was studied by using UV-DRS spectrophotometer (Perkin Elmer). TEM image was recorded on CM-200 (Philips) using The B-E-T method

and is used to determine surface area using Quantochrome Autosorb Automated Gas sorption system.

**Photocatalysis** In the present work photodegradation of Erioglaucine dye was studied in presence of nanocrystalline  $\text{SrCO}_3$ . Three kinds of experiments were carried out. In the first experiment 50 ml, 20 ppm solution of Erioglaucine dye solution was irradiated in a photoreactor using 0.5 gm of  $\text{SrCO}_3$  photocatalyst. The second experiment was carried out in absence of light. In the third experiment, only Erioglaucine dye solution without catalyst was irradiated with visible light. The lowering in absorbance due to degradation of dye was noted on double beam UV-Visible spectrophotometer (systronics) after each 30 min intervals. For a complete study on degradation of Erioglaucine dye, 0.5 gm of photocatalyst with 50 ml of 20 ppm dye solution under constant environment was taken.

## Results and Discussion

**General** Figure 1 reveals IR spectrum of the obtained  $\text{SrCO}_3$  product. The IR spectrum shows bands around  $3503$  and  $3344\text{ cm}^{-1}$ , confirming the stretching mode of an O-H group of surface water [31]. The support for the presence of  $\text{CO}_3^{2-}$  in the  $\text{SrCO}_3$  sample can be confirmed by its fingerprint peaks of  $D_{3h}$  symmetry at  $1432$ ,  $858.43$  and  $705\text{ cm}^{-1}$  for prepared  $\text{SrCO}_3$  sample to the vibrational modes  $\nu_3(E')$ ,  $\nu_2(A''_2)$  and  $\nu_4(E'')$  respectively. The peak appearing at  $1598\text{ cm}^{-1}$  is due to the bending mode of adsorbed water molecules [32].

The crystal phase of synthesised  $\text{SrCO}_3$  was checked XRD pattern (Fig.2). The observed  $2\theta$  values along with sharp diffraction pattern with intense peaks confirm the best crystallinity of the product. Observed peaks in the XRD pattern can be indexed as a pure cubic phase of  $\text{SrCO}_3$  and it well matches with JCPDS data card number 32-2476.

The XRD pattern shows no impurity peaks were detected. Further Debye-Scherrer equation was used to calculate particle size [33],  $D = 0.9 \lambda / \beta \cos \theta$ , Where,  $\lambda$ ,  $\beta$ ,  $\theta$  are the wavelength (X-ray), FWHM and Bragg's diffraction angle. The measured crystal dimension was found to be 98 nm using this XRD analysis.

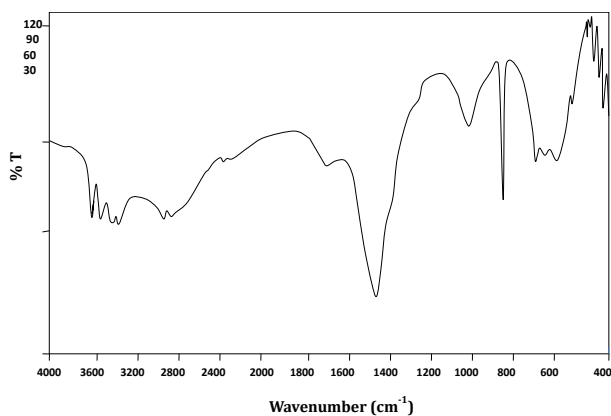


Fig. 1. FTIR spectrum of SrCO<sub>3</sub> nanoparticles

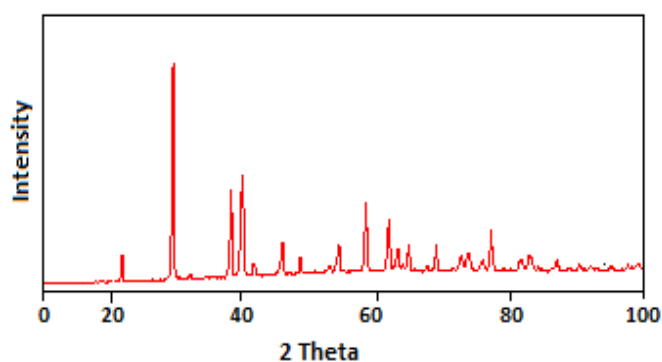


Fig. 2. XRD powder pattern of SrCO<sub>3</sub> nanoparticles

Figure 3 shows UV-DRS spectrum of SrCO<sub>3</sub>. The obtained UV-DRS shows absorption cut off at 300 nm. The band gap energy (E<sub>g</sub>) is obtained by the famous equation  $E = hc / \lambda$ .

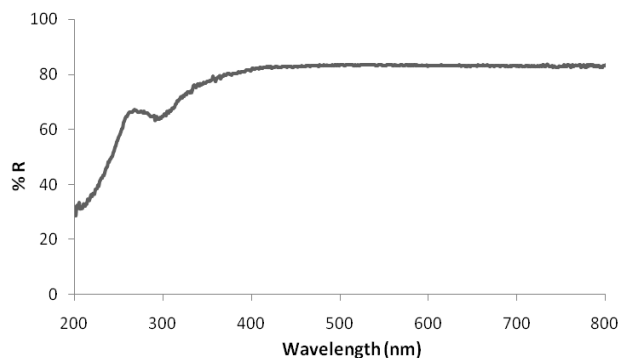


Fig. 3. UV-DRS spectrum of SrCO<sub>3</sub> nanoparticles

Using this equation the estimated band gap energy obtained is 4.1 eV. This calculated E<sub>g</sub> for SrCO<sub>3</sub> shows that it may possess an excellent photocatalytic activity. The surface morphology of the as-synthesized SrCO<sub>3</sub> semiconductor crystal was investigated with SEM. Figure 4 shows a typical image of the SEM of the synthesised SrCO<sub>3</sub> product. Using SEM technique it was found that, the strontium carbonate shows few particles are big, some of the short rod likes and most of them are agglomerated. The EDAX analysis confirms the stoichiometric composition taken during analysis.

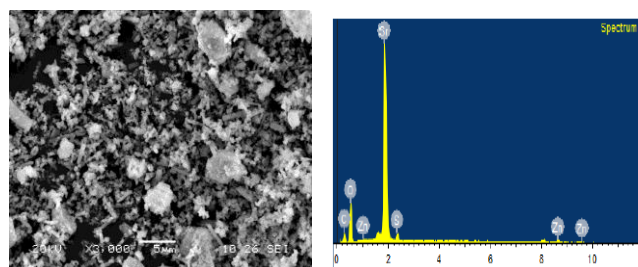


Fig. 4. SEM and EDAX analysis of SrCO<sub>3</sub> nanoparticles

TEM images (Fig 5) shows some of the crystals are cubic and rod-like. The SAED pattern along with TEM shows the cubic SrCO<sub>3</sub> structure and is fully conformable with XRD data. The particle dimensions evaluated by TEM for SrCO<sub>3</sub> are 98 nm.

Figure 6 depicts N<sub>2</sub> adsorption /desorption isotherm for synthesised SrCO<sub>3</sub>. It shows that the synthesised strontium carbonate has satisfied IV N<sub>2</sub> adsorption/ desorption isotherm with H1 hysteresis which indicates that sample is mesoporous in nature. The surface area (S<sub>BET</sub>) estimated by this method was found to be 178.9 m<sup>2</sup>/g, 0.105 cc/g and 54.37 Å<sup>0</sup> are the pore volume (V<sub>p</sub>) and pore diameter (d<sub>pm</sub><sup>2</sup>/g).

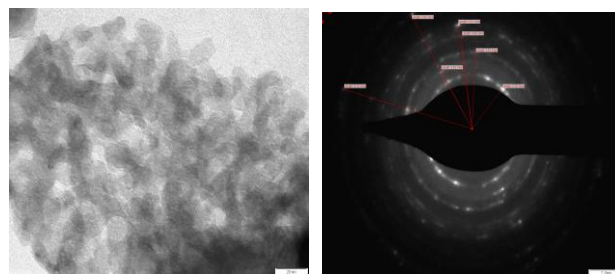
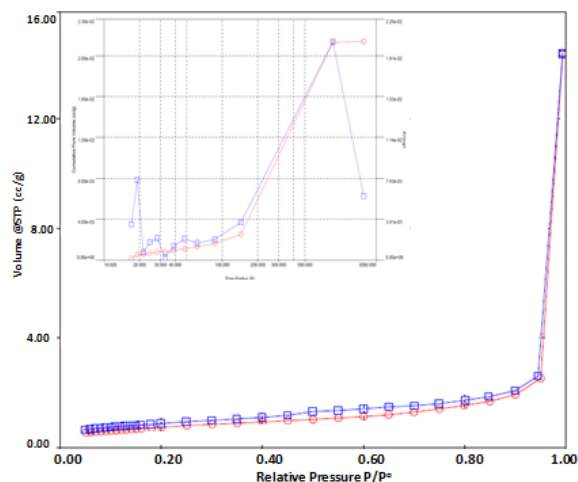
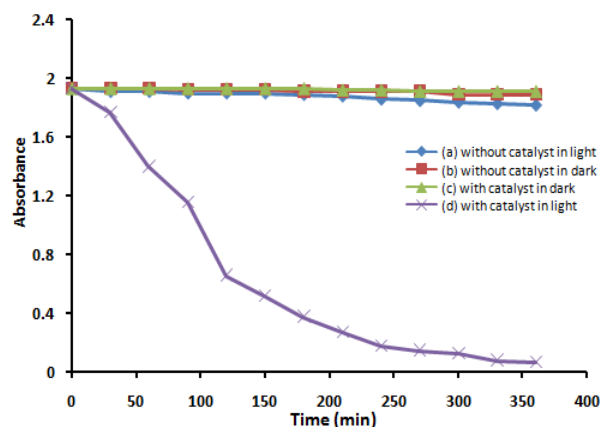


Fig. 5. TEM and SAED analysis of SrCO<sub>3</sub> nanoparticles.



**Fig. 6.** BET Surface area and Pore volume of  $\text{SrCO}_3$  nanoparticles.

**Photocatalytic activity of  $\text{SrCO}_3$**  Photocatalytic property of  $\text{SrCO}_3$  was investigated by photodegradation of Erioglaucine dye. The photodegradation of dye was evaluated by recording the absorbance using double beam spectrophotometer at 30 min. intervals. Figure 7 represents the photodegradation of Erioglaucine dye using  $\text{SrCO}_3$ , when irradiated with visible light. Figure 7 (curve a) depicts no effect on absorbance and hence very minute decrease in absorbance when the dye solution was irradiated with visible light in absence of photocatalyst.



**Fig. 7.** Effect of catalyst and light irradiation on dye degradation

Figure 7 (b and c) indicates there is no effect on absorbance due to presence or absence of catalyst in dark on dye degradation. Further Fig. 7, (curve d) indicates the rapid degradation of dye in presence of catalyst in light. This degradation occurs due to rise in the amount of catalyst that enhances ejection rate of photons and electrons in the conduction and valence band.

**Initial dye concentration effect** the photocatalytic degradation of Erioglaucine dye with various initial concentrations in the range of 10 to 50 ppm was investigated as a function of visible light irradiation time with natural pH of suspension with the loading of 0.5 gm  $\text{SrCO}_3$  in 100 ml dye solution (Fig. 8).

A careful inspection of Fig. 8 reveals that as the amount of Erioglaucine dye increases the rate of degradation of the dye shows a smaller rise initially and then decreases gradually. It was mentioned that at a lower amount of the dye, the photocatalytic reaction rate is nearly proportional to the dye concentration [34].

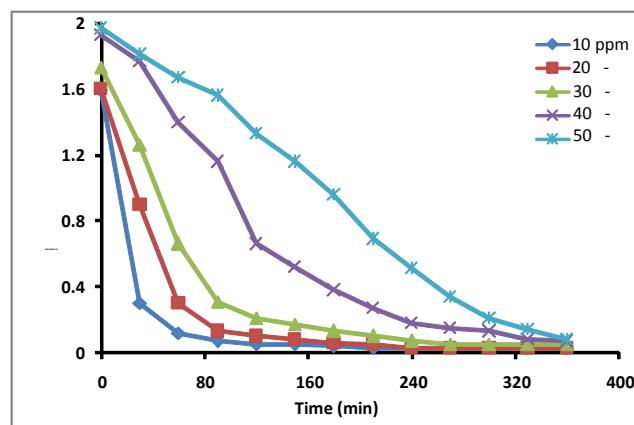


**Fig.8** Effect of concentration of dye solution on degradation using  $\text{SrCO}_3$

This is due to the fact that, when the concentration of dye exceeds an optimum value, the light penetration decreases through solution thus decreasing, thus reducing the absorption of the photon on  $\text{SrCO}_3$  catalyst. Due to adsorption of dye on the photoactive surface of a catalyst there occurs a decrease in active sites. The present study reveals that, with an increase in dye concentration up to

the certain range, the photocatalytic activity goes on decreasing. The lower range concentration of Erioglaucine used in the present study is 10 ppm.

*Effect of amount of catalyst* the amount of catalyst is an important factor for the study of photodegradation. Figure 9 shows a variation of the amount of catalyst (0.1 to 0.7 g) at a constant concentration of dye solution (10 ppm) at neutral pH. At low catalytic concentration, the degradation rate is diminishing because less number of surface active sites are available. With rising dose of catalyst, the degradation efficiency increases. On excess addition of photocatalyst the photons are get scattered from its surface and hence degradation rate diminishes. In this work, the minimum addition of  $\text{SrCO}_3$  nanoparticles was found to be 0.5 gm per 100 ml. Figure 10 reveals that the degradation of dye before and after exposure to the visible light and photocatalyst. It is observed that with increasing time of irradiation, the chromophoric absorption peak at 625 nm completely diminishes dark colorization of Erioglaucine solution. The colour of solution (absorbance 625 nm) decreased remarkably reaching a discoloration. Figure 10 confirms that within 120 min the absorbance reaches to zero in presence of nanocrystalline  $\text{SrCO}_3$ .

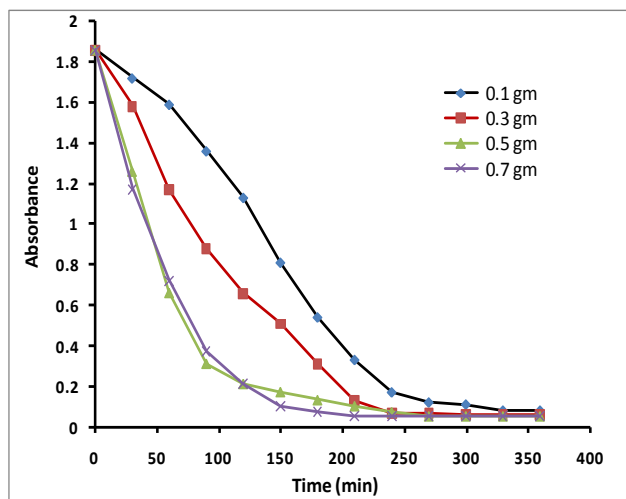


Fig. 9 Effect of amount of  $\text{SrCO}_3$  catalyst on dye degradation.

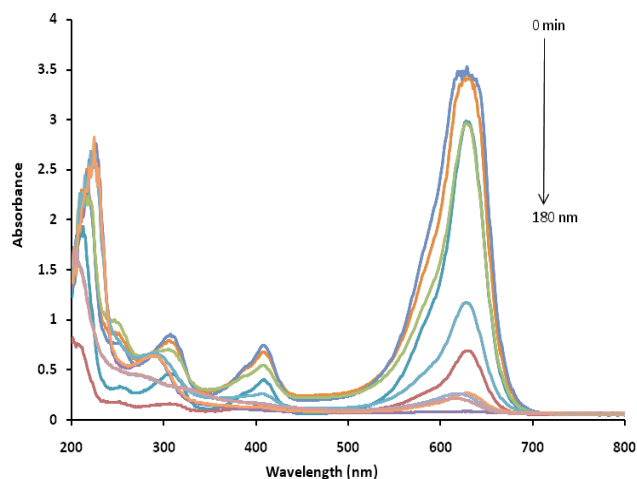


Fig. 10 UV-Visible spectrum of dye before and after degradation.

*LC-MS of degraded Erioglaucine dye* The mechanism for degradation of Erioglaucine dye was established by using Liquid Chromatography- Mass Spectroscopy (LC-MS). The LC-MS recorded for complete degraded Erioglaucine is shown in Fig. 11. The major Erioglaucine dye degradation pathway is represented in Fig.12. The structure of the different product was suggested on the basis of HPLC-MS fragmentations.

In the present molecule peaks of Erioglaucine dye observed at 792 m/z before irradiation only parent dye present as expected. Several fragments at 102 m/z, 121 m/z, 135m/z, 223 m/z, 277 m/z and 466 m/z that occurs after the degradation of dye.

*Recyclability of  $\text{SrCO}_3$  for degradation of Erioglaucine dye* The recyclability of  $\text{SrCO}_3$  was checked for degradation of Erioglaucine dye over five runs (Fig.13), after every use, the photocatalyst was washed with ethanol and dried at  $50^\circ\text{C}$  and redistributed in the fresh dye solution. The  $\text{SrCO}_3$  catalyst showed favourable reusability after five times recycling. We did observe some extent of catalytic loss during each run, this may cause a decrease in degradation.

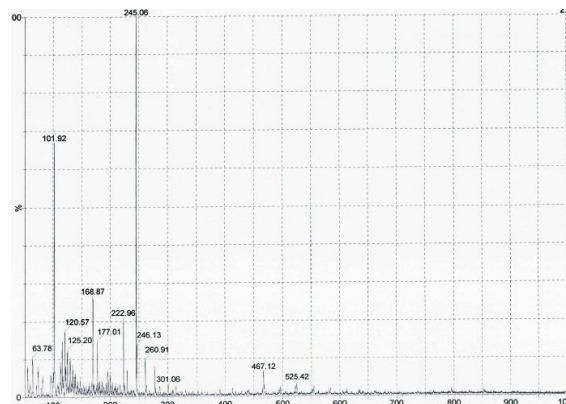


Fig. 11. LC-MS of the degraded dye solution.

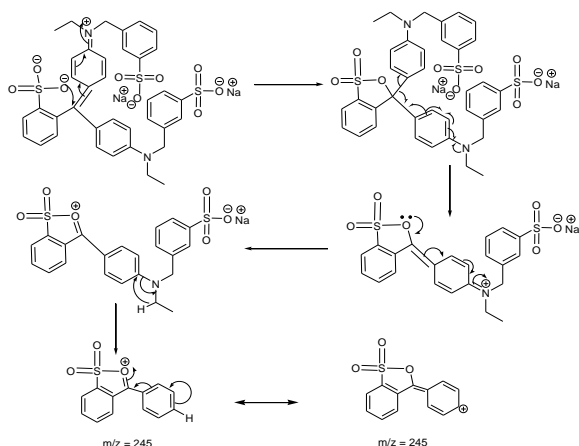


Fig. 12. Degradation mechanism of Erioglaucine dye.

## Conclusions

Visible light driven  $\text{SrCO}_3$  nanocrystalline photocatalyst was successfully synthesised by hydrothermal precipitation method. Experimental results obtained indicate that visible light illumination of the Erioglaucine dye solutions degrades to a greater extent. Further this work give evidence for development and design of new green mineralisation of dye and hence purification of water.

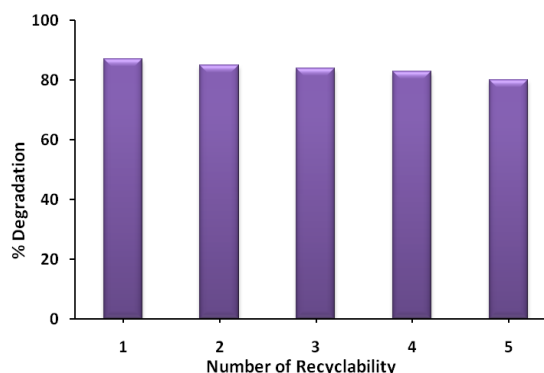


Fig.13 Recyclability of  $\text{SrCO}_3$  for degradation of Erioglaucine dye.

## Acknowledgements

The authors are grateful to CSIR, New Delhi and BCUD, S. P. Pune University, Pune for financial assistance and also thankful to IIT, Mumbai for their support for characterization.

## References

1. R. Ganesh, G.D. Boardman, *Water Res.*, 1994, **28**, 1367.
2. A. Yadav, S. Neraliya, A. Gopesh, *J. Env. Biol.*, 2007, **28**, 159.
3. A.V. Borhade, Y.R. Baste, *J. Therm. Anal. Calorim.*, 2012, 107, 77.
4. S. Chakrabarti, B.K. Datta, *J. Hazard. Mat.*, 2004, **112**, 269.
5. Y. Xu, J. Jia, D. Zhang, Y. Wang, *Chem. Engg. J.*, 2009, **150**, 302.
6. Y.S. Chen, J.C. Crittenden, S. Hackney, L. Sutter, D.W. Hand, *Environ. Sci. Technol.*, 2005, **39**, 1201.
7. M. N. Rashad El, A.A. Amin, *Int. J. Phy. Sci.*, 2007, **2**, 73.
8. A.D. Paola, E.G. Lopez, S. Ikeda, L. Palmisano, *Catal. Today*, 2002, **75**, 87.
9. M.A. Rauf, M.A. Meetani, S. Hisaindee, *Desalination*, 2011, **276**, 13.
10. V.A. Sakkas, A. Islam Md, C. Stalikas, T.A. Albanis, *J. Hazard. Mat.* 2010, **175**, 33.
11. A.V. Borhade, D.R. Tope, S.G. Gite, *Arab. J. Chem.*, DOI.Org/10.1016/j.arabjc.2012.11.001.
12. A.V. Borhade, D.R. Tope, B.K. Uphade, *Res. Chem. Intermed.*, 2012, **40**(1) 211.



13. A.V. Borhade, K.G. Kanade, D.R. Tope, M.D. Patil, *Res. Chem. Intermed.*, DOI 10.1007/s11164-012-0515-z (2012).
14. A.V. Borhade, Y. R. Baste, *Arab. J. Chem.*, DOI.org.10.1016/j. Arabic.2012.10.001.
15. H. Liu, T. Peng, D. Ke, Z. Peng, C. Yan, *Mater. Chem. Phys.*, 2007, **104**, 377.
16. S.M. Teleb, D.El. Sayed, E.M. Nour. *Bull. Mater. Sci.*, 2004, **27**, 483.
17. M.S. Refat, AL-Qahatant, *Bull Mater. Sci.*, 2011, **34**, 853.
18. S. Lee, K. Cho, Y. Son, *Thin solid film*, 2012, **524**, 290.
19. M. V. Nassar, I. S. Ahmed, *Polyhedron*, 2011, **30**, 2431.
20. A. V. Radha, A. Narrotsky, *American Minerologist*, 2004, **99**, 1063.
21. M. Mohamed, Al-Majthouba , S. Moamen, B. Refata, *Adv. Appl. Sci. Res.*, 2012, **3** 183.
22. K. Omata, N. Nukui, T. Hottai, Y. Showa, M. Yamad, *Catal. Commun.*, 2014, **5**, 755.
23. J. Kuther, G. Nells, R. Sheshadri, M. Schaub. H.J. Butt, W, Tremel, *Chem. Eur. J.*, (9), 1834.
24. D. Rautaray, S.R. Sainkar, M. Sastry, *Langmuir*, 2003, **19**(3), 888.
25. L. Qi, K. Xi, Ma, *J. Acta Chemica Sinica*, 2003, **61**(1), 126.
26. J.Aizenberg, A. J. Black, G.M. Whitesides, *J. Am. Chem. Soc.*, 1999, **121**, 4500.
27. J. Kuther, M. Bartz, R. Sheshadri, G.B.M. Vaughanc , W. Tremala , *J. Mater. Chem.*, 2001,**11**, 503.
28. J. Kuther, R. Sheshadri, W .Tremel, *Chem. Int.Ed.*, 1998, **37**, 3044.
29. S.Z. Li, H. Zhang , J. Xu, D.R. Yang, *Mater. Lett.*, 2005, 59, 420.
30. Q. Huang, L. Gao, Y. Cai, F. Aldinger, *Chem. Lett.*, 2004, **33**, 290.
31. A. Askarinejad, A. Morsali, *Chem. Eng. J.*, 2009, **150**, 569.
32. K.T. Ehlssissen, Vidal A. Delahaya, P. Genin, M. Figlarz, P. Willmann, *J. Mater. Chem.*, 1993, 3, 883.
33. J. Feng, H.C. Zeng, *Nanocubes Chem. Mater.*, 2003 **15**, 2829.
34. I.K. Konstantinou, T.A. Albanis, *Appl Catal.B. Environ.*, 2004, **49**, 1.